

# Magnetic Properties of Wood Treated with Nano-magnetite and Furfuryl Alcohol Impregnation

Irma Wahyuningtyas,<sup>a</sup> Istie Rahayu,<sup>a,\*</sup> Akhiruddin Maddu,<sup>b</sup> and Esti Prihatini<sup>a</sup>

The impregnation of jabon wood (*Anthocephalus cadamba* Miq.) with a magnetic compound can increase the quality of the wood. In this study, magnetic woods were made using the *ex situ* impregnation of jabon woods with nano-magnetite (Fe<sub>3</sub>O<sub>4</sub>). The objective of this study was to analyze the characteristics of jabon magnetic wood. Two other impregnation solutions were also used in this study: (1) water (untreated) and (2) furfuryl alcohol plus nano-magnetite. The physical properties of magnetic jabon wood were improved compared with untreated wood, as shown by the results of the characterization tests. Scanning electron microscopy with energy-dispersive X-ray spectroscopy showed nano-magnetite in the micropores of magnetic jabon wood. The results of the Fourier-transform infrared spectroscopy showed chemical bonding between the wood polymer and the furan ring and Fe-O functional groups. The X-ray diffraction results showed a decrease in the degree of crystallinity as the concentration of nano-magnetite increased. The magnetic properties were tested *via* vibrating-sample magnetometry and the FA-Fe<sub>3</sub>O<sub>4</sub>-treated wood showed the highest magnetization.

DOI: 10.15376/biores.17.4.6496-6510

Keywords: Fast-growing wood; Furfuryl alcohol; Magnetic wood; Nano-magnetite; Nanoparticles

Contact information: a: Department of Forest Products, IPB University; b: Department of Physics, IPB University, Bogor 16680 Indonesia; \*Corresponding author: [istiesr@apps.ipb.ac.id](mailto:istiesr@apps.ipb.ac.id)

## INTRODUCTION

Jabon (*Anthocephalus cadamba* Miq.) is a fast-growing wood species that is harvested at an age of 4 to 5 years. Because of its rapid growth, this tree has a high juvenile wood content, resulting in low-rated physical and mechanical properties (Krisnawati *et al.* 2011; Rahayu *et al.* 2014). Consequently, this wood is only used as raw material for light construction, plywood, wood flooring, *etc.* (Prihatini *et al.* 2020). An innovation that could expand the function of jabon wood is to make it magnetic and impart good physical properties.

Magnetic wood that is used for furniture or building construction can absorb electromagnetic wave radiation from electronic devices (Oka *et al.* 2009; Oka *et al.* 2012). Wood can be made magnetic by both *in situ* and *ex situ* methods. The *in situ* method was successfully carried out by Dong *et al.* (2016) through a chemical coprecipitation process within the wood, using a precursor of Fe<sub>3</sub>O<sub>4</sub> (nano-magnetite). Oka and Fujita (1999) successfully made magnetic wood with various *ex situ* methods, *e.g.*, impregnation, coating, and mixing nanoparticles with sawdust, and then made boards (Oka *et al.* 2000, 2002, 2004). The *ex situ* method is easier because it uses magnetic materials that are already nanometer-sized. The overall process is faster than the *in situ* method, in which the magnetic material is synthesized in the wood.

Nano-magnetite has a high iron content; this compound is superparamagnetic and sensitive to external magnetic fields (Abadi *et al.* 2016). Nanoparticles are effective for treating wood because of their high dispersion, distribution, and penetration, as well as their low viscosity (Fufa and Hovde 2010; Teng *et al.* 2018). However, nano-magnetite is difficult to dissolve in water, and it readily undergoes coagulation, aggregation, and oxidation. Furthermore, it can easily wash out of wood due to low interaction with wood polymers (Kumar *et al.* 2010). These problems can be overcome through the addition of furfuryl alcohol (FA) as a dispersant.

Furfuryl alcohol, which has strong polarity, is an environmentally friendly organic chemical made from agricultural waste (Lande *et al.* 2004; Tathod and Dhepe 2015; Teng *et al.* 2018). As a dispersant, FA forms a colloidal phase with nano-magnetite and protects its stability, causing it to not agglomerate. The colloids can penetrate deeper into the wood and increase the magnetic properties of the magnetic wood (Kumar *et al.* 2010; Teng *et al.* 2018). Furfuryl alcohol also reduces the degradation of magnetic wood due to acids and alkalis (Lande *et al.* 2004; Forest Product Laboratory 2010; Dong *et al.* 2016). Previously, FA-impregnated wood has been produced for flooring, furniture, and light construction usage (Hill 2006; Treu *et al.* 2009; Dong *et al.* 2014; Hazarika and Maji 2014). Dong *et al.* (2016) also impregnated poplar wood using nano-magnetite followed by furfurylation to obtain its dimensional and magnetic stability. In this study, magnetic jabon wood was obtained through *ex situ* modification, using the nano-magnetite and FA impregnation method. The objective of this study was to analyze the characteristics of jabon magnetic wood.

## EXPERIMENTAL

### Materials

Defect-free 5-year-old jabon wood was obtained from Bogor, West Java, Indonesia. The samples of wood were cut to dimensions of 2 cm × 2 cm × 2 cm, according to BS 373 (1957), before treatment and the subsequent testing of the physical properties of the magnetic wood. The chemicals used were nano-magnetite (diameter 297 nm ± 5 nm; Nanjing Aocheng Chemical Co., China), FA (98% purity, Sigma Aldrich Pte. Ltd. China), and demineralized water.

### Methods

#### *Preparation of impregnation solution*

Three impregnation solutions were used in this study: demineralized water, nano-magnetite 7.5%, and FA (1 mol to 1 mol ratio) with nano-magnetite (7.5%). The solutions were mixed using a magnetic stirrer for 15 min, and then a Cole-Parmer sonicator was used at an amplitude of 40% for 30 min to form homogeneous solutions.

#### *Impregnation process*

The impregnation process was adapted from Oka *et al.* (2012), Dong *et al.* (2016), and Rahayu *et al.* (2020). First, the samples were dried at 103 ± 2 °C until they reached a constant weight. Each sample was immersed in an impregnation solution in an impregnation tube under 0.5 bar vacuum for 2 h, followed by being under a 1 bar pressure for 2 h. After impregnation, the samples were wrapped in aluminum foil and kept at 65 °C

for 12 h for polymerization. Afterward, the aluminum foil was removed, and the samples were oven-dried at  $103 \pm 2$  °C. Each treatment consisted of 10 samples.

#### *Testing the physical properties of magnetic jabon wood*

The physical properties and dimensional stability of magnetic jabon wood were tested according to Rowell and Ellis (1978), Hill (2006), and Bowyer *et al.* (2007). The testing included weight percent gain (WPG), leachability ( $L$ ), anti-swelling efficiency (ASE), water uptake (WU), and density ( $\rho$ ). The WPG and leachability were calculated using Eqs. 1 and 2,

$$\text{WPG (\%)} = [(W_1 - W_0)/W_0] \times 100 \quad (1)$$

$$L (\%) = [(W_1 - W_2)/(W_1 - W_0)] \times 100 \quad (2)$$

where  $W_0$  is the oven-dry weight of the sample before the impregnation treatment,  $W_1$  is the oven-dry weight after the impregnation treatment, and  $W_2$  is the oven-dry weight of the sample after immersion in water for 24 h. The ASE was calculated according to Eq. 3,

$$\text{ASE (\%)} = [(S_u - S_t)/S_t] \times 100 \quad (3)$$

where  $S_u$  is the volume shrinkage of the untreated sample that was immersed in water at room temperature for 24 h, and  $S_t$  is the volume shrinkage of the treated samples. The WU was evaluated after the samples were immersed in water for 24 h and were calculated according to Eq. 4,

$$\text{WU (\%)} = [(W_2 - W_1)/W_1] \times 100 \quad (4)$$

where  $W_1$  is the oven-dry weight of the sample after the impregnation treatment, and  $W_2$  is the sample weight after being immersed in water for 24 h. The bulking effect (BE) was calculated according to Eq. 5,

$$\text{BE (\%)} = [(V_1 - V_0)/V_0] \times 100 \quad (5)$$

where  $V_0$  is the dry volume of the sample before the impregnation treatment, and  $V_1$  is the dry volume sample after the impregnation treatment. The density was calculated after the treatment according to Eq. 6,

$$\rho (\text{g/cm}^3) = W_1/V_1 \quad (6)$$

where  $W_1$  is the oven-dry weight of the sample after the impregnation treatment, and  $V_1$  is the volume dry sample after the impregnation treatment.

#### *Scanning electron microscopy and energy-dispersive x-ray spectroscopy*

The morphology of the wood cell wall after the impregnation treatment was analyzed using scanning electron microscopy (SEM) (JSM-6510LA, JEOL Ltd, Tokyo, Japan). Samples were cut to the dimensions of 0.5 cm  $\times$  0.5 cm  $\times$  0.5 cm in the tangential section, sputter-coated with gold, and analyzed at a voltage of 15 kV. Afterward, energy-dispersive X-ray spectroscopy (EDX) analysis was done to determine the chemical content of the jabon wood samples.

#### *Fourier transform infrared spectrometry*

Fourier-transform infrared spectrometry (FT-IR) (Thermo Scientific, Nicolet 6700, Waltham, MA) was used to qualitatively analyze the functional groups of the three types of jabon wood samples. The samples were separately milled to a powder size of 200-mesh

and embedded in potassium bromide pellets. The scans were from 400 to 4000  $\text{cm}^{-1}$  at a 4  $\text{cm}^{-1}$  resolution for 32 scans.

#### *X-ray diffraction analysis*

The degree of crystallinity of the jabon wood samples was analyzed by X-ray diffraction (XRD) (Empyrean, Malvern Panalytical, Malvern, UK). The samples were cut to a thickness of 2 mm on the tangential plane. The parameters used in this analysis were as follows: a Cu anode, a 40 kV voltage, a 30 mA electric current, and a scan range  $2\theta$  between  $5^\circ$  and  $70^\circ$  with a scanning speed of 0.0263  $^\circ/\text{step}$ .

#### *Vibrating sample magnetometry*

The magnetic properties of the jabon wood samples were analyzed *via* vibrating sample magnetometry (VSM) (VSM DEXING type 250, CN) at 300 K in an external magnetic field from 100 Oe to 21 kOe. The dimensions of the sample used were 3.8 mm  $\times$  3.8 mm  $\times$  1.5 mm in the longitudinal plane. The parameters used in this analysis were as follows: magnetization saturation (Ms), retentivity (Mr), and coercivity (Hc).

#### *Data analysis*

The data were analyzed using a completely randomized design and the effect of the impregnation treatment on the physical properties of the jabon wood samples was evaluated *via* analysis of variance (ANOVA). The differences between the treatments were analyzed using Duncan's multiple range test at a 1% level of accuracy. The software used for data analysis was IBM SPSS Statistics (version 25.0, IBM, Armonk, NY).

## RESULTS AND DISCUSSION

### Physical Properties of Magnetic Jabon Wood

The average of the physical properties with the standard deviation of the treated jabon wood is shown in Table 1. The results showed slight increases in the WPG, BE, and density of jabon wood treated with  $\text{Fe}_3\text{O}_4$ , which were not significantly different from the untreated wood. This outcome was likely due to the characteristics of the nano-magnetite particles, which are insoluble in pure water, and the suspected agglomeration of nano-magnetite particles occurring on the wood surface. However, because the magnetite particles used in this research were of nanometer size, the physical properties of jabon wood increased to a slight extent. The most important physical property of the material that will affect solubility is particle size. In the case of crystals smaller than 1  $\mu\text{m}$ , the high surface area may increase solubility (Cornell and Schwertmann 2006).

**Table 1.** Physical Properties of Untreated and Treated Jabon Wood

Wood Treatment	WPG (%)	BE (%)	$\rho$ ( $\text{g}/\text{cm}^3$ )	L (%)	ASE (%)	WU (%)
Untreated	0.00 <sup>a</sup>	1.11 $\pm$ 0.49 <sup>a</sup>	0.27 $\pm$ 0.02 <sup>a</sup>	0.00 <sup>a</sup>	0.00 <sup>a</sup>	138.37 $\pm$ 7.62 <sup>c</sup>
$\text{Fe}_3\text{O}_4$	4.37 $\pm$ 0.62 <sup>a</sup>	1.37 $\pm$ 1.12 <sup>a</sup>	0.28 $\pm$ 0.01 <sup>a</sup>	63.63 $\pm$ 5.37 <sup>b</sup>	31.50 $\pm$ 4.90 <sup>b</sup>	134.10 $\pm$ 9.98 <sup>c</sup>
FA- $\text{Fe}_3\text{O}_4$	47.73 $\pm$ 6.57 <sup>b</sup>	7.38 $\pm$ 1.38 <sup>b</sup>	0.39 $\pm$ 0.01 <sup>b</sup>	11.37 $\pm$ 6.09 <sup>a</sup>	77.51 $\pm$ 5.53 <sup>c</sup>	55.47 $\pm$ 8.15 <sup>b</sup>

Note: <sup>a, b, c, d</sup> the result of Duncan's multiple range tests

These phenomena can cause the size of the nano-magnetite particles to increase and thus block the wood pores, thereby preventing the nano-magnetite from penetrating deeper into the wood (Liu *et al.* 2001). It occurs because the surface free energy of magnetite is relatively high (Cornell and Schwertsmann 2006).

The addition of FA to the nano-magnetite treatment caused the WPG, BE, and density to significantly increase compared with the untreated wood. The presence of FA is thought to replace bound water in the cell walls. Furthermore, the polymerization process also causes the FA molecules to undergo *in situ* polycondensation to form the polymer resins in the cell walls of the jabon wood and thus improve its physical properties (Bi *et al.* 2021). From Table 1, the penetration of solution, namely FA and nano-magnetite, affected the physical properties and dimensional stability of jabon wood. Treatment with FA and nano-magnetite caused the wood to have improved anti-swelling properties, which was indicated by a significant increase in the ASE and a decrease in the WU in the FA-Fe<sub>3</sub>O<sub>4</sub> wood samples. Nano-magnetite creates tortuous paths within the wood cell wall, thereby limiting the interaction between the wood polymer and water molecules. Furfuryl alcohol, which has hydrophobic properties, also agglomerates and clogs cell cavities, reducing the occurrence of chemical bonds with water.

The FA-Fe<sub>3</sub>O<sub>4</sub> magnetic jabon wood had a significantly lower leaching rate than the Fe<sub>3</sub>O<sub>4</sub> magnetic jabon wood. The addition of FA to the impregnation solution was thought to reduce the migration of magnetic nanoparticles in jabon wood, such that only a small amount of leaching may occur (Dong *et al.* 2014; Dong *et al.* 2016; Farah *et al.* 2021). The authors' previous research (Rahayu *et al.* 2022), showed that WPG (47.44%), BE (7.13%) and ASE (64.26%) values of treated jabon wood by the *in situ* method (NaOH precursor) were similar to FA-Fe<sub>3</sub>O<sub>4</sub> treated jabon wood. It was concluded that FA as a dispersant was capable of maintaining good dispersion, making it possible to deposit nano Fe<sub>3</sub>O<sub>4</sub> into jabon wood.

### Scanning Electron Microscopy (SEM) and Energy Dispersive X-ray Spectroscopy (EDX)

The morphology of the jabon wood after treatment is shown in Fig. 1. The cell cavities of the untreated wood appeared empty and are not covered by chemicals (Fig. 1a). Furthermore, the Fe<sub>3</sub>O<sub>4</sub>-treated wood also showed no nanoparticle deposits in the cell wood cavities (Fig. 1c). Therefore, the addition of the colloid-forming FA-Fe<sub>3</sub>O<sub>4</sub> caused morphological changes in the cell cavities of the jabon wood (Fig. 1d). In these samples, the cell cavities were covered and saturated with FA-Fe<sub>3</sub>O<sub>4</sub>, and nano-magnetite sedimentation occurred on the surface of the jabon wood. The nano-magnetite that could not enter the lumen of the wood cells aggregated, thus reducing the high surface energy of nano-magnetite (Choat *et al.* 2008; Garskaite *et al.* 2021).

The presence of nano-magnetite in the wood cavity was also confirmed *via* EDX analysis, and the results are shown in Table 2. Based on the data described in Table 2, the amount of nano-magnetite contained in the impregnated jabon wood increased when FA was added to the impregnation solution. The FA-Fe<sub>3</sub>O<sub>4</sub> colloid can fill the space in the wood cell wall and cover the wood cell cavity, thereby reducing the hygroscopicity of the wood. According to Dirna *et al.* (2020), the presence of nanoparticles in the impregnation solution can improve the physical properties of wood. As such, this study found that FA-Fe<sub>3</sub>O<sub>4</sub> magnetic jabon wood showed the best results among all treatments.

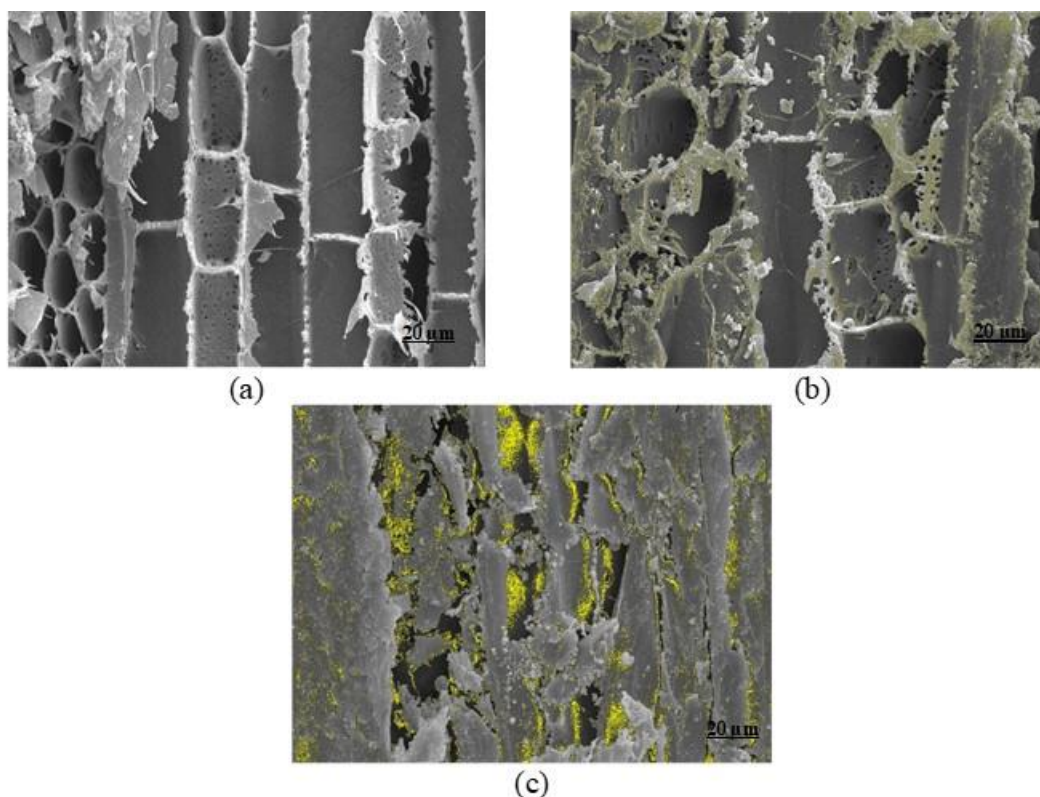


**Fig. 1.** Morphology of the (a) untreated; (b)  $\text{Fe}_3\text{O}_4$ , and (c) FA- $\text{Fe}_3\text{O}_4$  jabon wood treated (at a magnification of  $\times 550$ )

**Table 2.** Chemical Composition of Untreated dan Treated Jabon Wood with  $\text{Fe}_3\text{O}_4$  and FA- $\text{Fe}_3\text{O}_4$

Wood Sample Treatment	C (wt%)	O (wt%)	Fe (wt%)
Untreated	$59.37 \pm 2.71$	$40.63 \pm 14.14$	0.00
$\text{Fe}_3\text{O}_4$	$58.50 \pm 3.50$	$31.94 \pm 14.24$	$9.56 \pm 13.01$
FA- $\text{Fe}_3\text{O}_4$	$50.72 \pm 1.44$	$22.14 \pm 3.79$	$27.14 \pm 3.85$

### Fourier-transform Infrared Spectrometry (FT-IR) Analysis

The functional groups of the jabon wood are shown in Fig. 2. The analysis detected O-H bending of the cell wall component at a wavenumber of  $3340 \text{ cm}^{-1}$  (Hazarika and Maji 2014). According to Nandiyanto *et al.* (2019), the O-H stretching of the hydroxyl group ranges from  $3570 \text{ cm}^{-1}$  to  $3200 \text{ cm}^{-1}$ , while Cheng *et al.* (2013) stated that a peak at  $3400 \text{ cm}^{-1}$  indicated a water molecule in the liquid phase. In addition, the analysis found a peak at a wavenumber of  $2906 \text{ cm}^{-1}$ . This peak indicated the presence of the vibration of the C-H stretching functional group, based on previous research by Gan *et al.* (2017), who detected the C-H functional group at a wave number of  $2908 \text{ cm}^{-1}$ .

The functional group vibration at a wavenumber of  $1730 \text{ cm}^{-1}$  is C=O stretching (Coates 2006). This is assigned to the C=O stretching in non-conjugated ketones and ester groups, which could be due to the cleavage of ester linkages in hemicelluloses as well as the cleavage of lignin side chains by the magnetic treatment (Dong *et al.* 2016; Hazarika and Maji 2014). The FA polymerization was also followed by the appearance of a peak at  $1595 \text{ cm}^{-1}$ , which indicated the presence of a 2,4-substituted furan ring structure vibration (Pranger *et al.* 2012; Dong *et al.* 2016). The furan ring also caused a weakening of the peak

of the C-O functional group at  $1030\text{ cm}^{-1}$  (Rahayu *et al.* 2021). The peak of the Fe-O vibration from the nano-magnetite samples appeared at a wavenumber of  $548\text{ cm}^{-1}$ . The Fe-O peak of the  $\text{Fe}_3\text{O}_4$  wood sample appeared at a wavenumber of  $563\text{ cm}^{-1}$ , while it shifted to  $560\text{ cm}^{-1}$  in the FA- $\text{Fe}_3\text{O}_4$  sample. In a study by Lin and Ho (2014), a strong peak of the Fe-O group of bulk nano-magnetite was detected at a wavenumber of  $580\text{ cm}^{-1}$  and a weak peak was detected at a wavenumber of  $436\text{ cm}^{-1}$ .

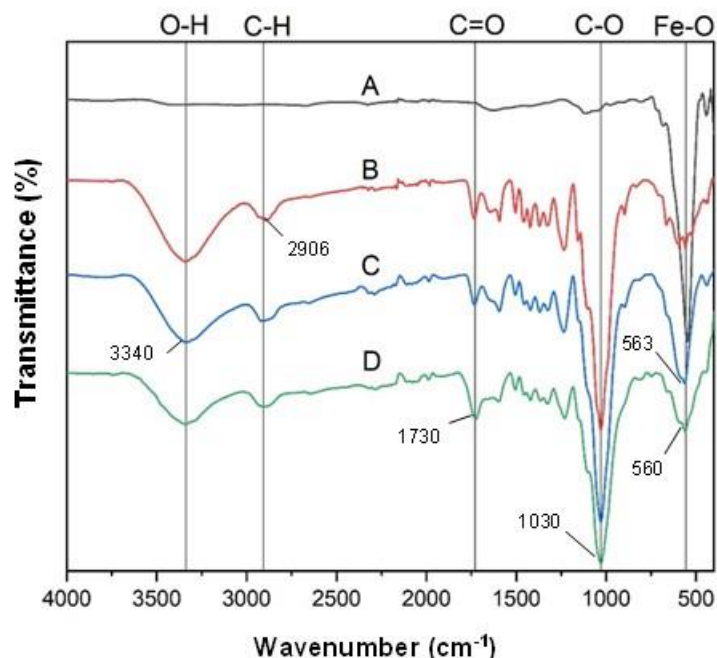


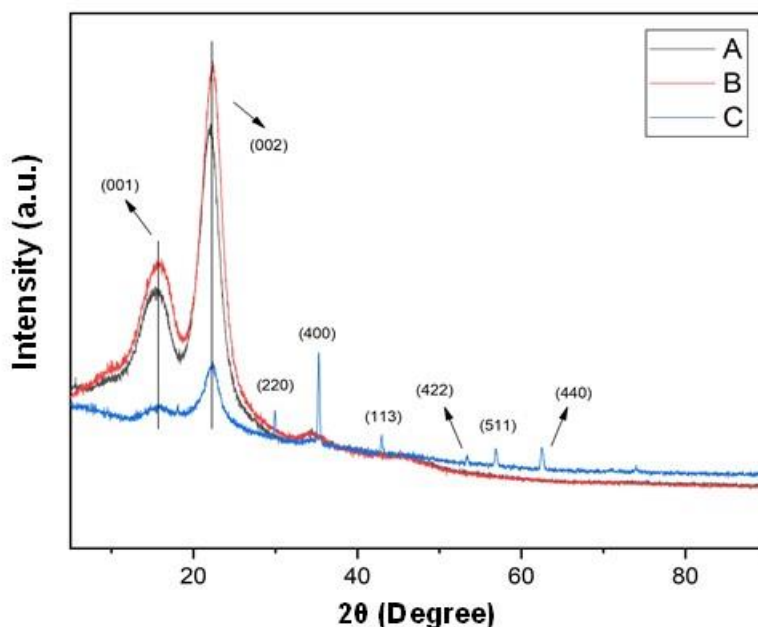
**Fig. 2.** FT-IR spectra of (a) nano-magnetite; (b) untreated; and treated jabon wood with (c)  $\text{Fe}_3\text{O}_4$ ; (d) FA- $\text{Fe}_3\text{O}_4$

### XRD Analysis

The XRD spectra of untreated and treated jabon wood with  $\text{Fe}_3\text{O}_4$ , and FA- $\text{Fe}_3\text{O}_4$  are shown in Fig. 3. The degree of crystallinity of  $\text{Fe}_3\text{O}_4$  treated wood increased compared to untreated wood. It was due to the restructuration of cellulose in the amorph phase when it interacted with water (Dong *et al.* 2014) as a dispersant of  $\text{Fe}_3\text{O}_4$ . The degree of crystallinity of FA- $\text{Fe}_3\text{O}_4$  jabon wood decreased with the addition of nano-magnetite and FA, significantly different from untreated and  $\text{Fe}_3\text{O}_4$  treated wood (Table 3). The  $\text{Fe}_3\text{O}_4$ -treated wood had a higher crystallinity than the untreated wood. This result was thought to be because of the presence of water-insoluble nano-magnetite, which blocked cavities within the wood and prevented water from penetrating deeper into the wood. As a result, the crystallinity of the jabon wood remained higher. According to Xu and Huang (2011), treatment with FA- $\text{Fe}_3\text{O}_4$  causes the oxidation of jabon wood cellulose. Nano-magnetite and FA can react with cellulose in the wood cell wall and weaken the intermolecular hydrogen bonds. The compounds also open the pyranose ring, which breaks down and depolymerizes the crystal structure of jabon wood cellulose, thereby considerably reducing its crystallinity. Rahayu *et al.* (2021) stated that FA addition in ganitri wood can decrease the wood crystallinity. As shown in Fig. 3, the crystal planes  $I_{001}$  ( $15.7^\circ$  and  $16.04^\circ$ ) and  $I_{002}$  ( $22.36^\circ$ ) indicate the cellulose from jabon wood (Lionetto *et al.* 2012; Dong *et al.* 2016).

**Table 3.** Degree of Crystallinity of Untreated and Treated Jabon Wood with  $\text{Fe}_3\text{O}_4$ , and FA- $\text{Fe}_3\text{O}_4$ 

Wood Sample Treatment	Degree of Crystallinity (%)	Size of $\text{Fe}_3\text{O}_4$ inside jabon wood (nm)
Untreated	42.32	61.30
$\text{Fe}_3\text{O}_4$	45.99	65.26
FA- $\text{Fe}_3\text{O}_4$	29.98	43.18

**Fig. 3.** XRD spectra of untreated and treated jabon wood with  $\text{Fe}_3\text{O}_4$ , FA, and FA- $\text{Fe}_3\text{O}_4$ 

The effect of the addition of FA in magnetic jabon wood is indicated by the widened intensity in the peaks of  $I_{001}$  and  $I_{002}$ , which indicated that the crystalline cellulose area in jabon wood had become amorphous (Rahayu *et al.* 2021). In addition, a new peak was also found at  $2\theta = 18.14^\circ$  ( $I_{101}$ ), which was attributed to the formation of a crystalline area of cellulose. The peaks of  $2\theta = 29.95^\circ$  ( $I_{220}$ ),  $35.31^\circ$  ( $I_{311}$ ),  $42.98^\circ$  ( $I_{400}$ ),  $53.38^\circ$  ( $I_{422}$ ), and  $56.88^\circ$  ( $I_{511}$ ) were associated with the presence of  $\text{Fe}_3\text{O}_4$  that forms a crystalline area. According to Garskaite *et al.* (2021), the interaction of the colloidal impregnation solution with the wood cell wall components did not affect the stability of the nano-magnetite.

The sizes of  $\text{Fe}_3\text{O}_4$  inside jabon wood (Table 3), were determined based on an XRD diffractogram by using Scherrer equation (Hargreaves 2016). The size of  $\text{Fe}_3\text{O}_4$  inside FA- $\text{Fe}_3\text{O}_4$  treated wood (43.18 nm) was lower than  $\text{Fe}_3\text{O}_4$  treated (65.26 nm) and untreated (61.30 nm). This indicated that  $\text{Fe}_3\text{O}_4$  inside treated and untreated jabon wood could be regarded as nano-sized. Khan *et al.* (2019) stated that particles are classified as nano-sized if the size is within the range of 1 to 100 nm (by crystal size approach).

### Characterization of the Magnetic Properties

Figure 4 shows the apparent hysteresis behavior of the magnetic jabon wood. The direction of the magnetic moment of the wood was one-way magnetized and required a small external field. The hysteresis loop of the magnetic jabon wood obtained also had an elongated and narrow shape. According to Tang and Fu (2020), the loop shape indicated



paramagnetic behavior, which is characterized by saturation magnetization ( $M_s$ ), magnetization remanence ( $M_r$ ), and coercivity ( $H_c$ ) (Matsumoto *et al.* 2010; Gan *et al.* 2017). The  $M_s$ ,  $M_r$ , and  $H_c$  values are shown in Table 4. Untreated and FA-treated wood were not tested because there was no addition of nano-magnetite.

**Table 4.** Saturation Magnetization ( $M_s$ ), Retentivity ( $M_r$ ), and Coercivity ( $H_c$ ) of the Treated Jabon Wood

Wood Sample	$M_s$ (emu/g)	$M_r$ (emu/g)	$H_c$ (Oe)
$Fe_3O_4$	0.20	0.07	1.21
FA- $Fe_3O_4$	1.89	0.27	2.79

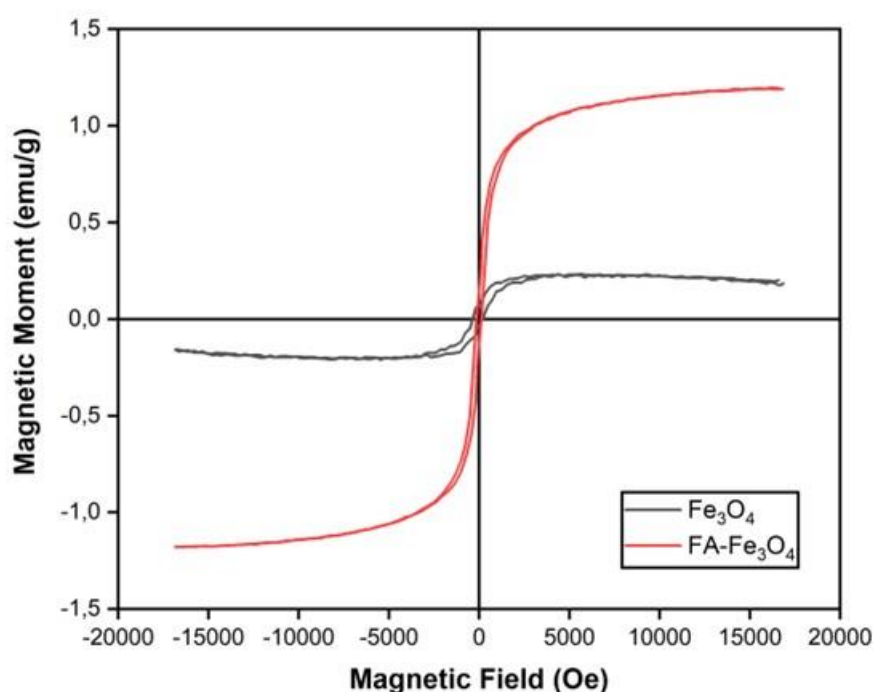


**Fig 4.** The magnetic hysteresis curve of the jabon wood treated with (a)  $Fe_3O_4$ ; and (b) FA- $Fe_3O_4$

The  $M_s$  value generated from this research was relatively low. However, the  $M_s$  value of the FA- $Fe_3O_4$ -treated wood was higher than the  $M_s$  value of the  $Fe_3O_4$ -treated jabon wood, which indicated that it was easier to magnetize. The lower  $M_s$  value of the  $Fe_3O_4$ -treated wood could be because of the decomposition of nano-magnetite (Dong *et al.* 2016). The decreased crystallinity caused by the penetration of FA in the FA- $Fe_3O_4$ -treated wood was caused by the high  $M_s$  value. The  $M_s$  value is influenced by the structure of the material, the size of the nanoparticles, and the degree of crystallinity (Setiadi *et al.* 2013; Willard and Daniil 2013). Besides, it is also caused by the presence of a higher content of nano-magnetite in FA- $Fe_3O_4$  treated wood (proven by EDX results). The  $M_s$  value in this study showed a higher number compared to magnetic wood that was synthesized *in situ* by Rahayu *et al.* (2022), through chemical coprecipitation using the precursors of strong base (0.079 emu/g) and weak base (0.0730 emu/g). Therefore, the role of FA in this study is very important to facilitate the magnetization of wood. The increase in the  $M_s$  value could

also be caused by the partial superparamagnetism of the magnetite nanoparticles. In these particles, the magnetite has a core with ferromagnetic characteristics, and it is coated with a material consisting of cellulose that has diamagnetic properties (Nypelö 2022). In addition, the decreased  $M_s$  value compared to the bulk phase could also be due to the presence of wood and FA, as non-magnetic materials on the nano-magnetite surface reduce the magnetic interactions (Oliveira *et al.* 2018). The correlation between WPG and  $M_s$  shows in Fig. 5.

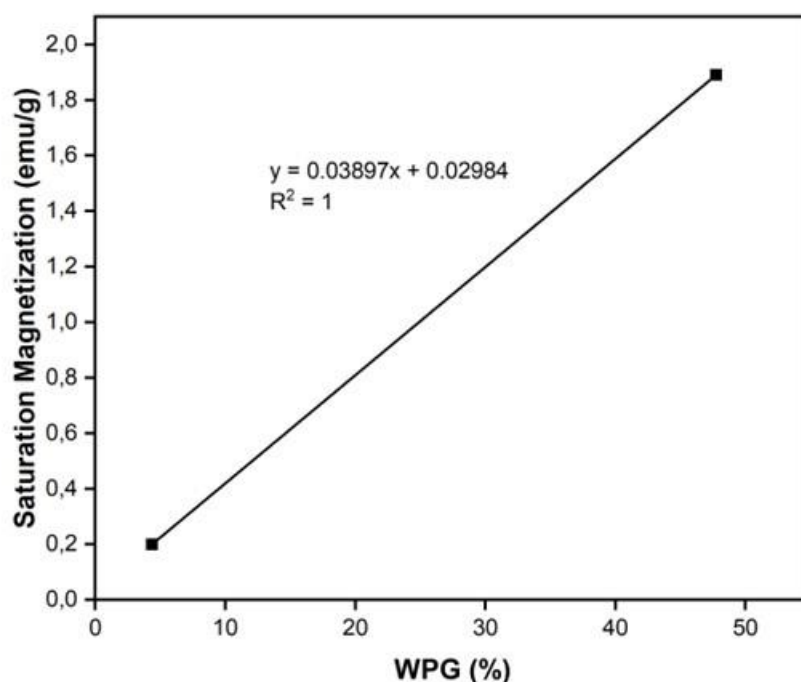


**Fig. 5.** The correlation between weight percent gain (WPG) and saturation magnetization ( $M_s$ ) of the magnetic jabon wood

The WPG showed a linear correlation with the  $M_s$  value, which means the more WPG increases, the greater value of  $M_s$  obtained. This was also shown by the research of Dong *et al.* (2016). Previous research conducted by Gan *et al.* (2017) stated that the  $M_s$  value of bulk nano-magnetite particles was 58.8 emu/g. Therefore,  $M_s$  values of  $Fe_3O_4$  and FA- $Fe_3O_4$ -treated wood are considered lower than  $M_s$  of bulk nano-magnetite. FA- $Fe_3O_4$ -treated wood is classified as soft magnetic material. The  $M_r$  value also showed an increase after the addition of FA, which means the magnetic properties of the wood were getting better. The  $M_r$  value shows the magnetic field remaining in the wood samples after the external magnetic field is removed. Moya *et al.* (2022) stated that the  $M_r$  value of magnetic wood *in situ via* coprecipitation method made from several tropical wood species ranged from 0.01 to 0.25 emu/g, which is slightly lower than the results of this study. This case may be caused by the influence of FA which reduces the crystallinity of the wood.

The higher  $H_c$  value in the FA- $Fe_3O_4$ -treated wood indicated that a stronger field was needed to remove the remanent magnetization. In addition, the structure of the wood can also affect its magnetic properties. Compared to the *in situ* method by Dong *et al.* (2016), the  $H_c$  value of magnetic wood in this study was higher and increased after adding FA to the solutions. Consequently, the nano-magnetite could be well distributed. The higher  $H_c$  value can also be explained by additional nanoparticles being present in the

composite and the difficulty of demagnetizing (Fliegans *et al.* 2021). Synthesis of magnetized biomass has been carried out on bamboo using  $\text{Fe}_3\text{O}_4$  combined with several chemicals *in situ*. This approach has been used to produce bamboo with good physical and mechanical properties, thermal stability, and absorbance of electromagnetic waves, making it suitable for structural applications (Lou *et al.* 2021; 2022a; 2022b).

## CONCLUSIONS

1. Impregnation treatment with nano-magnetite and furfuryl alcohol (FA) was successfully carried out to create magnetic jabon wood with good physical properties. Increases in the weight percentage gain (WPG), bulking effect (BE), density, and anti-swelling efficiency (ASE) were observed. In addition, the FA- $\text{Fe}_3\text{O}_4$  treatment led to decreases in the water uptake (WU) and leachability because of interactions between the wood cell wall polymers and the impregnation solutions, which reduced the ability of jabon wood to absorb water.
2. The presence of nano-magnetite in the jabon wood was demonstrated through scanning electron microscopy – energy dispersive X-ray (SEM-EDX) analysis and the amount of nano-magnetite was increased by adding FA to the impregnation solution. The Fourier transform infrared (FT-IR) analysis showed that furan rings and Fe-O functional groups were present in the treated wood. The degree of crystallinity of the jabon wood decreased after FA was added to the treatment because it induced amorphous properties. The vibrating sample magnetometry (VSM) analysis showed that the FA- $\text{Fe}_3\text{O}_4$ -treated wood had stronger magnetic properties compared to the  $\text{Fe}_3\text{O}_4$ -treated wood, as evidenced by a higher Ms.

## ACKNOWLEDGEMENTS

This research was funded by the Directorate General of Higher Education, Research, and Technology of the Ministry of Education, Culture, Research, and Technology of the Republic of Indonesia with the Postgraduate Research-Master Thesis Research scheme (PPS-PTM) (contract number 0277/E5/AK.04/2022 and 082/E5/PG.02.00.PT/2022) on 2022.

## REFERENCES CITED

- Abadi, M. T. H., Mufti, N., and Sunaryono, S. (2016). "Specific absorption rate (SAR) pada partikel nano Fe<sub>3</sub>O<sub>4</sub> dalam medan magnet AC, [Specific Absorption Rate (SAR) of Fe<sub>3</sub>O<sub>4</sub> nanoparticles in an AC magnetic field]" in: *Proceedings of the Seminar Nasional Fisika dan Pembelajarannya*, Nov. 25, Surabaya, Indonesia, pp. 248-254.
- Bi, W., Li, H., Hui, D., Gaff, M., Lorenzo, R., Corbi, I., Corbi, O., and Ashraf, M. (2021). "Effects of chemical modification and nanotechnology on wood properties," *Nanotechnol Reviews* 10(1), 978-1008. DOI: 10.1515/ntrev-2021-0065
- Bowyer, J. L., Shmulsky, R., and Haygreen, J. G. (2007). *Forest Products and Wood Science - An Introduction*, Blackwell Publisher, Hoboken, NJ.
- BS 373 (1957). "Standard methods of testing small clear specimens of timber," British Standards Institution, London, United Kingdom.
- Cheng, F., Cao, Q., Guan, Y., Cheng, H., Wang, X., and Miller, J. D. (2013). "FTIR analysis of water structure and its influence on the flotation of arcanite (K<sub>2</sub>SO<sub>4</sub>) and epsomite (MgSO<sub>4</sub>·7H<sub>2</sub>O)," *International Journal of Mineral Processing* 122, 36-42. DOI: 10.1016/j.minpro.2013.04.007
- Choat, B., Cobb, A. R., and Jansen, S. (2008). "Structure and function of bordered pits: New discoveries and impacts on whole-plant hydraulic function," *New Phytologist* Now 177(3), 608-626. DOI: 10.1111/j.1469-8137.2007.02317.x
- Coates, J. (2006). Interpretation of Infrared Spectra, A Practical Approach. In *Encyclopedia of Analytical Chemistry*. <https://doi.org/10.1002/9780470027318.a5606>
- Cornell, R., and Schwertmann, U. (2006). *The Iron Oxides: Structure, Properties, Reactions, Occurrences and Uses, 2nd, Completely Revised and Extended Edition* (2nd ed.). Wiley-VCH.
- Dirna, F. C., Rahayu, I., Zaini, L. H., Darmawan, W., and Prihatini, E. (2020). "Improvement of fast-growing wood species characteristics by MEG and nano SiO<sub>2</sub> impregnation," *Journal of the Korean Wood Science and Technology* 48(1), 41-49. DOI: 10.5658/WOOD.2020.48.1.41
- Dong, Y., Yan, Y., Zhang, S., and Li, J. (2014). "Wood/polymer nanocomposites prepared by impregnation with furfuryl alcohol and nano-SiO<sub>2</sub>," *BioResources* 9(4), 6028-6040. DOI: 10.15376/biores.9.4.6028-6040
- Dong, Y., Yan, Y., Zhang, Y., Zhang, S., and Li, J. (2016). "Combined treatment for conversion of fast-growing poplar wood to magnetic wood with high dimensional stability," *Wood Science and Technology* 50(3), 503-517. DOI: 10.1007/s00226-015-0789-6
- Farah, N. I. A., Zaidon, A., Anwar, U. M. K., Rabiatal-Adawiah, M. A., and Lee, S. H. (2021). "Improved performance of wood polymer nanocomposite impregnated with metal oxide nanoparticle-reinforced phenol formaldehyde resin," *Journal of Tropical Forest Science* 33(1), 77-87. DOI: 10.26525/jtfs2021.33.1.77
- Fliegans, J., Rado, C., Soulas, R., Guetaz, L., Tosoni, O., Dempsey, N. M., and Delette, G. (2021). "Revisiting the demagnetization curves of Dy-diffused Nd-Fe-B sintered magnets," *Journal of Magnetism and Magnetic Materials* 520, 1-28. DOI: 10.1016/j.jmmm.2020.167280
- Forest Product Laboratory (2010). *Wood Handbook: Wood as an Engineering Material*, Department of Agriculture Forest Service, Madison, WI.
- Fufa, S. M., and Hovde, P. J. (2010). "Nano-based modifications of wood and their environmental impact: Review," in: *Proceedings of the 11<sup>th</sup> World Conference on*

- Timber Engineering 2010*, 20-24 June, Trentino, Italy, pp. 2387-2388.  
[https://www.researchgate.net/publication/265111017\\_Nano-based\\_modifications\\_of\\_wood\\_and\\_their\\_environmental\\_impact\\_Review](https://www.researchgate.net/publication/265111017_Nano-based_modifications_of_wood_and_their_environmental_impact_Review).
- Gan, W., Gao, L., Xiao, S., Gao, R., Zhang, W., Li, J., and Zhan, X. (2017). "Magnetic wood as an effective induction heating material: Magnetocaloric effect and thermal insulation," *Advanced Materials Interfaces* 4(22), 1-9. DOI: 10.1002/admi.201700777
- Garskaite, E., Stoll, S. L., Forsberg, F., Lycksam, H., Stankeviciute, Z., Kareiva, A., Quintana, A., Jensen, C. J., Liu, K., and Sandberg, D. (2021). "The accessibility of the cell wall in Scots pine (*Pinus sylvestris* L.) sapwood to colloidal Fe<sub>3</sub>O<sub>4</sub> nanoparticles," *ACS Omega* 6(33), 21719-21729. DOI: 10.1021/acsomega.1c03204
- Hargreaves, J. (2016). "Some considerations related to the use of the Scherrer equation in powder X-ray diffraction as applied to heterogeneous catalysts," *Catalysis, Structure and Reactivity* 2, 33-37. <https://doi.org/10.1080/2055074X.2016.1252548>
- Hazarika, A., and Maji, T. K. (2014). "Modification of softwood by monomers and nanofillers," *Defence Science Journal* 64(3), 262-272. DOI: 10.14429/dsj.64.7325
- Hill, C. A. S. (2006). *Wood Modification: Chemical, Thermal, and Other Processes*, John Wiley and Sons Ltd, Hoboken, NJ.
- Khan, I., Saeed, K., and Khan, I. (2019). "Nanoparticles: Properties, applications and toxicities," *Arabian Journal of Chemistry* 12(7), 908-931. DOI: 10.1016/j.arabjc.2017.05.011
- Krisnawati, H., Kallio, M., and Kanninen, M. (2011). *Anthocephalus cadamba* Miq.: *Ecology, Silviculture and Productivity*. Center for International Forestry Research (CIFOR), Bogor Regency, Indonesia.
- Kumar, R., Inbaraj, B. S., and Chen, B. H. (2010). "Surface modification of superparamagnetic iron nanoparticles with calcium salt of poly( $\gamma$ -glutamic acid) as coating material," *Materials Research Bulletin* 45(11), 1603-1607. DOI: 10.1016/j.materresbull.2010.07.017
- Lande, S., Westin, M., and Schneider, M. (2004). "Properties of furfurylated wood," *Scan. J. Forest Research* 19(5), 22-30. DOI: 10.1080/0282758041001915
- Lin, C.-C., and Ho, J.-M. (2014). "Structural analysis and catalytic activity of Fe<sub>3</sub>O<sub>4</sub> nanoparticles prepared by a facile co-precipitation method in a rotating packed bed," *Cerametics International* 40(7, PART B) 10275-10282. DOI: 10.1016/j.ceramint.2014.02.119
- Lionetto, F., Sole, R. D., Cannoletta, D., Vasapollo, G., and Maffezzoli, A. (2012). "Monitoring wood degradation during weathering by cellulose crystallinity," *Materials* 5(10), 1910-1922. DOI: 10.3390/ma5101910
- Liu, Y., Yan, L., Heiden, P., and Laks, P. (2001). "Use of nanoparticles for controlled release of biocides in solid wood," *Journal of Applied Polymer Science* 79(3), 458-465. DOI: 10.1002/1097-4628(20010118)79:3<458::AID-APP80>3.0.CO;2-H
- Lou, Z., Han, X., Liu, J., Ma, Q., Yan, H., Y, C., Yang, L., Han, H., Weng, F., and Li, Y. (2021). "Nano-Fe<sub>3</sub>O<sub>4</sub>/bamboo bundles/phenolic resin oriented recombination ternary composite with enhanced multiple function," *Composites Part B: Engineering* 226. DOI: 10.1016/j.compositesb.2021.109335
- Lou, Z., Wang, Q., Kara U., I., Mamtani, R., S., Zhou, X., Bian, H., Yang, Z., Li, Y., Lv H., Adera, S., and Wang, Z. (2022a). "Biomass-derived carbon heterostructures enable environmentally adaptive wedeband electromagnetic wave absorbers," *Nano-Micro Letters* 14(11), 1-16. DOI: 10.1007/s40820-021-00750-z

- Lou, Z., Wang, Q., Sun, W., Liu, J., Yan, H., Bian, H., and Li, Y. (2022b). "Regulating lignin content to obtain excellent bamboo-derived electromagnetic wave absorber with thermal stability," *Chemical Engineering Journal* 430, article no. 133178. DOI: 10.1016/J.CEJ.2021.133178
- Matsumoto, Y., Teramoto, Y., and Nishio, Y. (2010). "Preparation of thermoplastic magnetic wood *via* etherification and *in-situ* synthesis of iron oxide," *Journal of Wood Chemistry and Technology* 30(4), 373-381. DOI: 10.1080/02773813.2010.523165
- Moya, R., Gait, J., Berrocal, A., and Merazzo, K., J. (2022). "*In situ* synthesis of Fe<sub>3</sub>O<sub>4</sub> nanoparticles and wood composite properties of three tropical species," *Materials* 15(3394), 1-17. DOI: 10.3390/ma15093394
- Nandiyanto, A. B. D., Oktiani, R., and Ragadhita, R. (2019). "How to read and interpret ftir spectroscopy of organic material," *Indonesian Journal of Science & Technology* 4(1), 97-118. DOI: 10.17509/ijost.v4i1.15806/
- Nypelo, T. (2022). "Magnetic cellulose: Does extending cellulose versatility with magnetic functionality facilitate its use in devices?" *Journal of Materials Chemistry C* 10(3), 805-818. DOI: 10.1039/d1tc02105b
- Oka, H., and Fujita, H. (1999). "Experimental study on magnetic and heating characteristics of magnetic wood," *Journal of Applied Physics* 85(8), 5732-5734. DOI: 10.1063/1.370267
- Oka, H., Fujita, H., and Seki, K. (2000). "Composition and heating efficiency of magnetic wood by induction heating," *IEEE Transactions on Magnetics* 36(5), 3715-3717. DOI: 10.1109/20.908950
- Oka, H., Hojo, A., Osada, H., Namizaki, Y., and Taniuchi, H. (2004). "Manufacturing methods and magnetic characteristics of magnetic wood," *Journal of Magnetism and Magnetic Materials* 272-276(3), 2332-2334. DOI: 10.1016/j.jmmm.2003.12.1214
- Oka, H., Hojo, A., Seki, K., and Takashiba, T. (2002). "Wood construction and magnetic characteristics of impregnated type magnetic wood," *Journal of Magnetism and Magnetic Materials* 239(1-3), 617-619. DOI: 10.1016/S0304-8853(01)00684-9
- Oka, H., Tanaka, K., Osada, H., Kubota, K., and Dawson, F. P. (2009). "Study of electromagnetic wave absorption characteristics and component parameters of laminated-type magnetic wood with stainless steel and ferrite powder for use as building materials," *J. Appl. Physics* 105(7), 2007-2010. DOI: 10.1063/1.3056403
- Oka, H., Terui, M., Osada, H., Sekino, N., Namizaki, Y., Oka, H., and Dawson, F. P. (2012). "Electromagnetic wave absorption characteristics adjustment method of recycled powder-type magnetic wood for use as a building material," *IEEE Transactions on Magnetics* 48(11), 3498-3500. DOI: 10.1109/TMAG.2012.2196026
- Oliveira, P. N., Bini, R. D., Dias, G. S., Alcouffe, P., Santos, I. A., David, L., and Cótica, L. F. (2018). "Magnetite nanoparticles with controlled sizes *via* thermal degradation of optimized PVA/Fe(III) complexes," *Journal of Magnetism and Magnetic Materials* 460, 381-390. DOI: 10.1016/j.jmmm.2018.04.005
- Pranger, L. A., Nunnery, G. A., and Tannenbaum, R. (2012). "Mechanism of the nanoparticle-catalyzed polymerization of furfuryl alcohol and the thermal and mechanical properties of the resulting nanocomposites," *Composites Part B: Engineering* 43(3), 1139-1146. DOI: 10.1016/j.compositesb.2011.08.010
- Prihatini, E., Maddu, A., Rahayu, I. S., Kurniati, M., and Darmawan, W. (2020). "Improvement of physical properties of jabon (*Anthocephalus cadamba*) through the impregnation of nano-SiO<sub>2</sub> and melamin formaldehyde furfuryl alcohol copolymer,"

- in: *Proceedings of the International Conference on Forest Products (ICFP) 2020: 12<sup>th</sup> International Symposium of IWORS*, 1 September, Bogor, Indonesia, pp. 1-9.
- Rahayu, I., Darmawan, W., Nugroho, N., Nandika, D., and Marchal, R. (2014). "Demarcation point between juvenile and mature wood in sengon (*Falcataria moluccana*) and jabon (*Antocephalus cadamba*)," *Journal of Tropical Forest Science* 26(3), 331-339.
- Rahayu, I., Darmawan, W., Zaini, L. H., and Prihatini, E. (2020). "Characteristics of fast-growing wood impregnated with nanoparticles," *Journal of Forestry Research* 31(2), 677-685. DOI: 10.1007/s11676-019-00902-3
- Rahayu, I., Pratama, A., Darmawan, W., Nandika, D., and Prihatini, E. (2021). Characteristics of impregnated wood by nano silica from betung bamboo leaves. *IOP Conference Series: Earth and Environmental Science*, 891, 12019. DOI: 10.1088/1755-1315/891/1/012019
- Rahayu, I., Prihatini, E., Ismail, R., Darmawan, W., Karlinasari, L., and Laksono, G. D. (2022). "Fast rowing magnetic wood synthesis by an in-situ method," *Polymers* 14(2137), 1-14. DOI: 10.3390/polym14112137
- Rowell, R. M., and Ellis, W. D. (1978). "Determination of dimensional stabilization of wood using the water-soak method," *Wood and Fiber* 10(2), 104-111.
- Setiadi, E. A., Shabrina, N., Retno, H., Utami, B., and Fahmi, N. F. (2013). "Sintesis nanopartikel cobalt ferrite ( $\text{CoFe}_2\text{O}_4$ ) dengan metode kopresipitasi dan karakterisasi sifat kemagnetannya [Synthesis of cobalt ferrite ( $\text{CoFe}_2\text{O}_4$ ) nanoparticles by coprecipitation method and characterization of their magnetic properties]," *Indonesian Journal of Applied Physics* 3(1), 55-62. DOI: 10.13057/ijap.v3i01.1216
- Tang, T., and Fu, Y. (2020). "Formation of chitosan/sodium phytate/nano- $\text{Fe}_3\text{O}_4$  magnetic coatings on wood surfaces *via* layer-by-layer self-assembly," *Coatings* 10(1), 1-8. DOI: 10.3390/coatings10010051
- Tathod, A. P., and Dhepe, P. L. (2015). "Efficient method for the conversion of agricultural waste into sugar alcohols over supported bimetallic catalysts," *Bioresource Technology* 178, 36-44. DOI: 10.1016/j.biortech.2014.10.036
- Teng, T.-J., Arip, M. N. M., Sudesh, K., Nemoikina, A., Jalaludin, Z., Ng, E.-P., and Lee, H.-L. (2018). "Conventional technology and nanotechnology in wood preservation: A review," *BioResources* 13(4), 9220-9252. DOI: 10.15376/biores.13.4.Teng.
- Treu, A., Pilgård, A., Puttmann, S., Krause, A., and Westin, M. (2009). "Material properties of furfurylated wood for window production," in: *Proceedings of the 40<sup>th</sup> Annual Meeting of the International Research Group on Wood Protection*, 24-28 May, Beijing, China. pp. 1-13. [https://www.researchgate.net/publication/228841654\\_Material\\_properties\\_of\\_furfurylated\\_wood\\_for\\_window\\_production](https://www.researchgate.net/publication/228841654_Material_properties_of_furfurylated_wood_for_window_production).
- Willard, M. A., smf Daniil, M. (2013). "Chapter Four - Nanocrystalline soft magnetic alloys two decades of progress," *Handbook of Magnetic Materials* 21, 173-342. DOI: 10.1016/B978-0-444-59593-5.00004-0
- Xu, Y. H., and Huang, C. (2011). "Effect of sodium periodate selective oxidation on crystallinity of cotton cellulose," *Advanced Materials Research* 197-198, 1201-1204. DOI: 10.4028/www.scientific.net/AMR.197-198.1201

Article submitted: May 8, 2022; Peer review completed: June 19, 2022; Revised version received: September 13, 2022; Accepted: September 14, 2022; Published: October 3, 2022. DOI: 10.15376/biores.17.4.6496-6510